J. Earth Planet. Sci. Nagoya Univ., Vol. 40, 1 to 16, 1993

240 Ma CHIME Ages of Monazite and Zircon from the Hirasawa Granitic Mass in the South Kitakami Terrane

Kazuhiro SUZUKI and Mamoru ADACHI

Department of Earth and Planetary Sciences, Nagoya University, Nagoya 464-01, Japan
(Received August 1, 1993 / Accepted October 20, 1993)

ABSTRACT

CHIME (chemical Th-U-total Pb isochron) ages were determined on monazite and zircon from three samples (Nos. 0708A, 0708B and 0709) of the Hirasawa granitic mass (Hirasawa Mass) in the South Kitakami terrane, Northeast Japan. The CHIME monazite ages are 240±20 Ma for sample 0708A, 240±10 Ma for sample 0708B and 240±10 Ma for sample 0709. Zircon from sample 0708A gives a CHIME age of 240±20 Ma. These age data indicate the late Permian to early Triassic emplacement of the Hirasawa Mass. Rocks of the Hirasawa Mass are coarse-grained peraluminous biotite adamellite, having ca. 74% SiO_2, 0.22% TiO_2, 13.8% Al_2O_3, 1.9% total Fe as FeO, 0.6% MgO, 1.5% CaO, 3.5% Na_2O and 4% K_2O. They are generally similar to other late Permian to early Triassic peraluminous granitoids in the South Kitakami terrane, but are discriminated from the 250–260 Ma leucocratic adamellite at Kusayami-zawa in higher CaO/(Na_2O+K_2O) ratios and from the 240–250 Ma leucogranite of the Okuhinotsuchi Mass in lower K_2O/Na_2O ratios and higher TiO_2 contents. The late Permian to early Triassic plutonism in the South Kitakami terrane, which was much extensive and diverse, corresponds to the major tectonic event between Permian and Triassic periods.

INTRODUCTION

There has been much dispute whether or not pre-Silurian or Precambrian basement exists in the South Kitakami terrane, Northeast Japan. The Hikami Granite and several small pre-Cretaceous granitoid masses (the Komatsu-pass, Shiroishi-pass, Yokamachi, Ezo, Hirasawa, Obata and Okuhinotsuchi Masses; Fig. 1) have been considered to be parts of pre-Silurian basement (e.g. Kitakami Paleozoic Research Group, 1982; Mori et al., 1992). It is rather surprising that a Carboniferous age (351±12 Ma Rb-Sr whole-rock isochron age for the Hikami Granite, Shibata, 1974) has long been ignored without any scientific refute. Our recent CHIME geochronology, however, confirmed Shibata's conclusion that the Hikami Granite is of early Carboniferous age (340–360 Ma CHIME monazite and zircon ages; Suzuki and Adachi, 1991a; Suzuki et al., 1992). We also disclosed that monazite-bearing leucocratic adamellite immediately below the "unconformity" at Kusayami-zawa, previously regarded as a variety of the Hikami granite (Murata et al., 1974), contains 240–250 Ma monazite and zircon (Suzuki et al., 1992). This was the first document to unveil the existence of the late Permian-early Triassic granite body in the South Kitakami terrane. Subsequently, we obtained latest Permian age of 250–260 Ma for magmatic monazite, zircon and xenotime from the Okuhinotsuchi Mass, about 15 km northwest of the Hikami Granite, although it has been regarded as pre-Silurian granite (Kitakami Paleozoic Research Group, 1982; Kawamura, 1983). The Okuhinotsuchi Mass contains xenocrysts of late Silurian to early Devonian zircon and/or Th-rich monazite as well (Adachi et al., in press).

Since granitoids of the Hirasawa Mass, like those of the Okuhinotsuchi Mass and at Kusayami-zawa, contain monazite, we expected that the Hirasawa Mass is also of late Permian to early Triassic age. In order to shed more light on the chronological history of the pre-Cretaceous plutonism in the South Kitakami terrane, we made CHIME age determinations of monazite and zircon from three granitoid samples of the Hirasawa Mass. In this paper we report the CHIME age result and discuss its geological meaning.

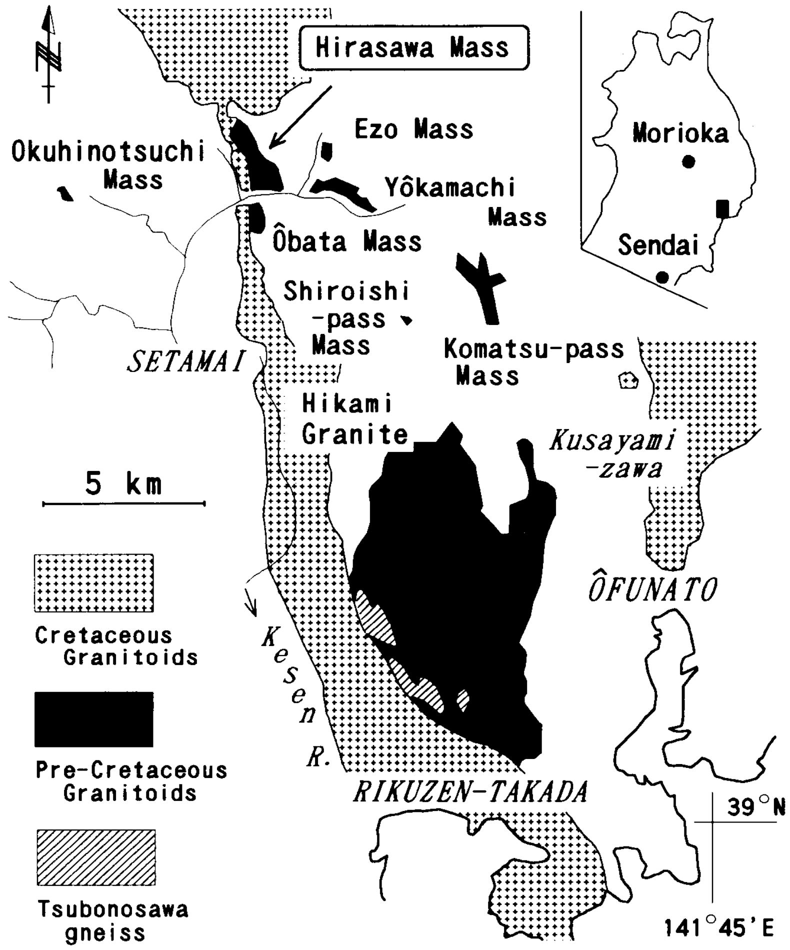

Fig. 1. Map showing the locality of the Hirasawa granitic mass, together with the distribution of pre-Cretaceous granitoid masses and Silurian Tsubonosawa gneiss in the South Kitakami terrane (simplified and slightly modified from Kitakami Paleozoic Research Group, 1982).

GEOLOGICAL OUTLINE AND DESCRIPTION OF SAMPLES

The Hirasawa Mass is exposed as an NNW-SSE trending small mass (about 3 km in length and 1 km in width) in the northern part of Arisu-cho, Kesen-gun, Iwate Prefecture (Fig. 2). The mass is bounded on the east and on the north by limestone of the Carboniferous Nagaiwa Formation, and intruded on the west by the Cretaceous Kesengawa Granodiorite (112 Ma K-Ar biotite age,

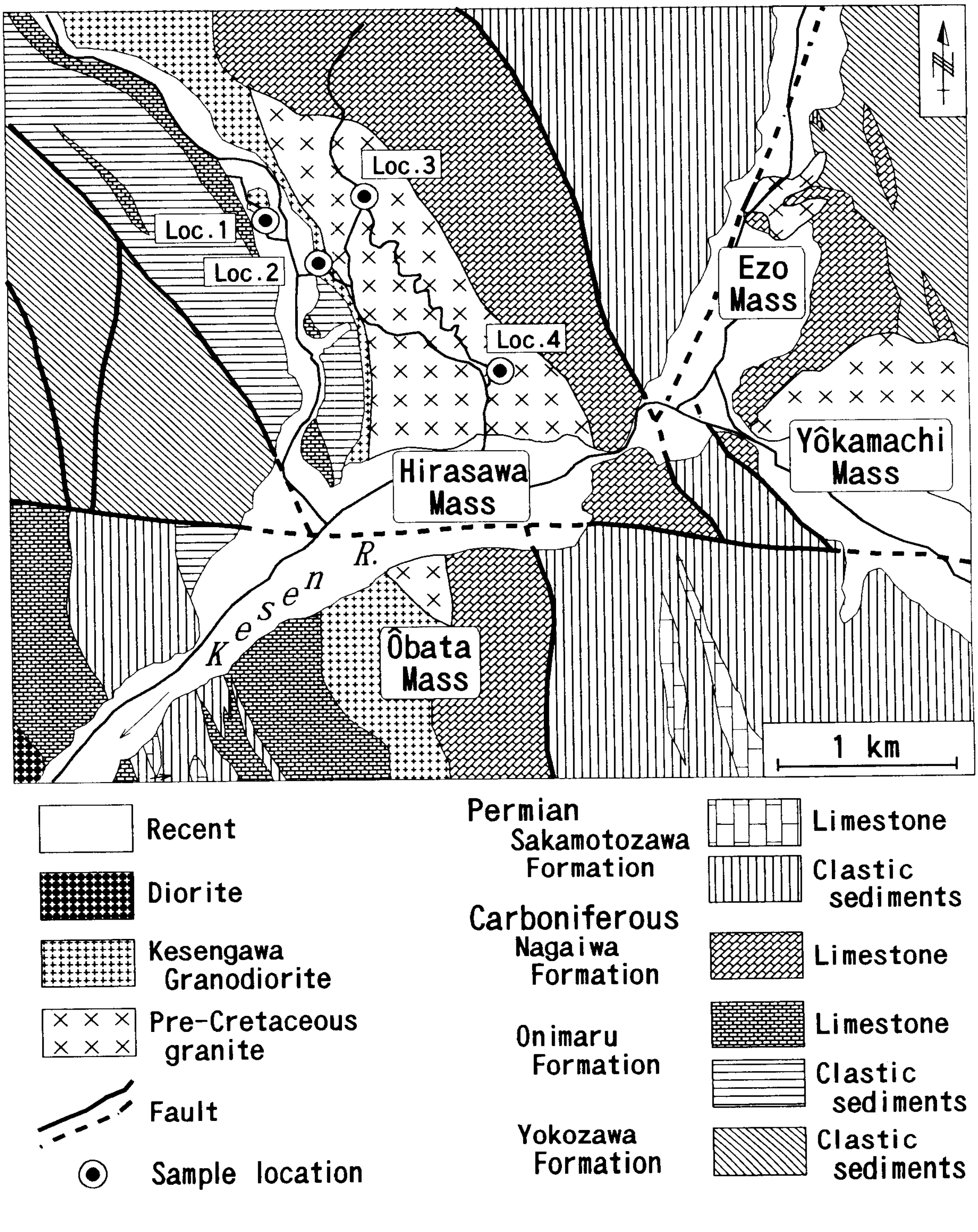

Fig. 2. Map showing sample locations of adamellite from the Hirasawa Mass and granodiorite from the Kesengawa Granodiorite (Geologic map after Metal Mining Agency of Japan, 1971)

Kawano and Ueda, 1964; 112±39 Ma Rb-Sr whole-rock isochron age, Shibata, 1974). Attempts to define the age of the Hirasawa Mass by examining the presence or absence of its contact metamorphism on the adjacent limestone have been unsuccessful, owing to the limited weathered outcrop and the thermal effect from the Kesengawa Granite.

Most parts of the Hirasawa Mass are highly weathered. Exceptionally fresh rocks, however, crop out on road-cuts in the northern part (Loc. 3). We collected two fresh samples from Loc. 3 and one saprolite sample from Loc. 4. Rocks at Loc. 3 exhibit partly a prominent gneissosity or sheared foliation due to parallel alignment of micaceous seams. It trends NNE-SSW direction and dips 70–80° to east.

One sample (No. 0708A) from Loc. 3 shows a distinct gneissose texture and the other (No. 0708B) shows a porphyritic texture with weak foliation. They are adamellite in composition and comprise quartz, oligoclase–andesine, microcline–microperthite, biotite and muscovite. Accessory minerals include apatite, zircon, monazite and iron ores (mainly ilmenite); magnetite and sphene are very rare or absent. Quartz and plagioclase are, at least in part, recrystallized to granular mosaic. Most K-feldspar grains in sample 0708B, ca. 12 mm in maximum size, remain unrecrystallized and are responsible for the porphyritic texture. Fine-grained recrystallized flakes of brown biotite aggregates together with muscovite make the micaceous seams. Zircon grains are euhedral, and some show concentric growth zoning. The length ranges from 0.08 to 0.35 mm, and the elongation (length/width) ratios concentrate around 2.2 (Fig. 3A). Monazite grains, 0.06–0.18 mm in size, are anhedral to subhedral and occur in unrecrystallized and recrystallied quartz and feldspar grains as well as mica flakes. These petrographic features suggest that the rocks at Loc. 3 were originally sheared and/or mylonitized adamellite which later underwent thermal metamorphism of the Cretaceous Kesengawa Granodiorite.

The saprolite, highly weathered granite, sample (No. 0709) from Loc. 4 does not show a distinct gneissose structure, although the coarse-grained porphyritic texture with weak foliation remains intact. This rock, like those from Loc. 3, contains both zircon and monazite. Zircon grains, 0.07–0.37 mm in length are euhedral and plotted in the nearly same field as those from Loc. 3 on the length vs. elongation diagram (Fig. 3A). A close similarity in zircon morphologies may be attributed to the cogenesis of rocks from Locs. 3 and 4.

Coarse-grained gneissose hornblende granodiorite (sample No. 0707A) cut by leucocratic hornblende granite vein (sample No. 0707B) occurs at Loc. 2, and medium-grained foliated hornblende granodiorite (sample No. 0706) occurs at Loc. 1; macroscopically samples 0707A and 0706 are similar to each other. These rocks are highly weathered and characterized by the presence of hornblende, sphene and magnetite and by the absence of monazite. As is clear from the mineralogical characteristics and zircon morphologies (Fig. 3), the foliated granodiorite and leucocratic hornblende granite at Locs. 1 and 2 are much different from samples from Locs. 3 and 4, and they may be regarded as varieties of the Kesengawa Granodiorite.

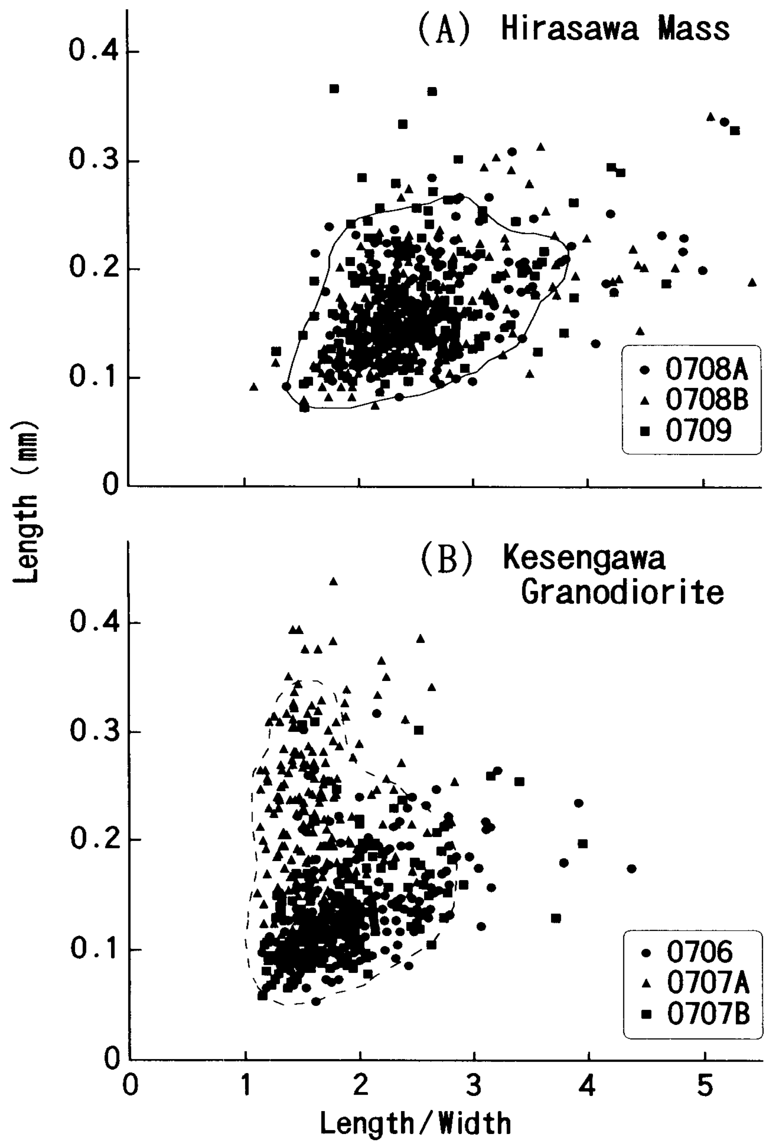

Fig. 3. Plots of length vs. elongation (length/width) for zircon grains from three adamellite samples (sample Nos. 0708A, 0708B and 0709) in the Hirasawa Mass (A) and two granodiorite samples (sample Nos. 0706 and 0707A) and a leucocratic granite sample (sample No. 0707B) in the Cretaceous Kesengawa Granodiorite (B). Solid and dashed lines in the figures represent 1 % contour of distribution intensity defined in an area of 0.4×0.04 scale units.

CHIME AGES OF MONAZITE AND ZIRCON

Since details of the experimental procedures (mineral separation, EPMA analysis and CHIME age calculation) have been described elsewhere (Suzuki et al., 1991, 1992; Suzuki and Adachi, 1991a,b; Adachi and Suzuki, 1992), the readers are requested to refer to them. Microprobe analyses of monazite and zircon are listed in Appendix 1; the detection limit of PbO at 2σ confidence level is 0.008—0.01 wt. %, and the relative error in the determination is 15—25% for 0.02 wt. % of the concentration.

Monazite contains 2.70−8.60% ThO_2 and 0.07−1.05% UO_2. Plots of PbO vs. ThO_2* for monazite grains from samples 0708A, 0708B and 0709 are given in Fig. 4. All data points of individual samples are arrayed linearly in the PbO-ThO_2* diagram. Data points for sample 0708A (solid circle), except that of grain M12 (open circle), give an isochron age of 240±20 Ma (MSWD=0.45) with an intercept value of −0.0006±0.0042, those for sample 0708B (triangle) an isochron age of 240±10 Ma (MSWD=0.16) with an intercept value of 0.0017±0.0020, and those for 0709 (square) an isochron age of 240±10 Ma (MSWD=0.15) with an intercept value of 0.0006±0.0020 (errors are of 2σ). If we combine all data points for three samples, we obtain a CHIME age of 240±10 Ma (MSWD=0.24) with an intercept value of 0.0008±0.0010.

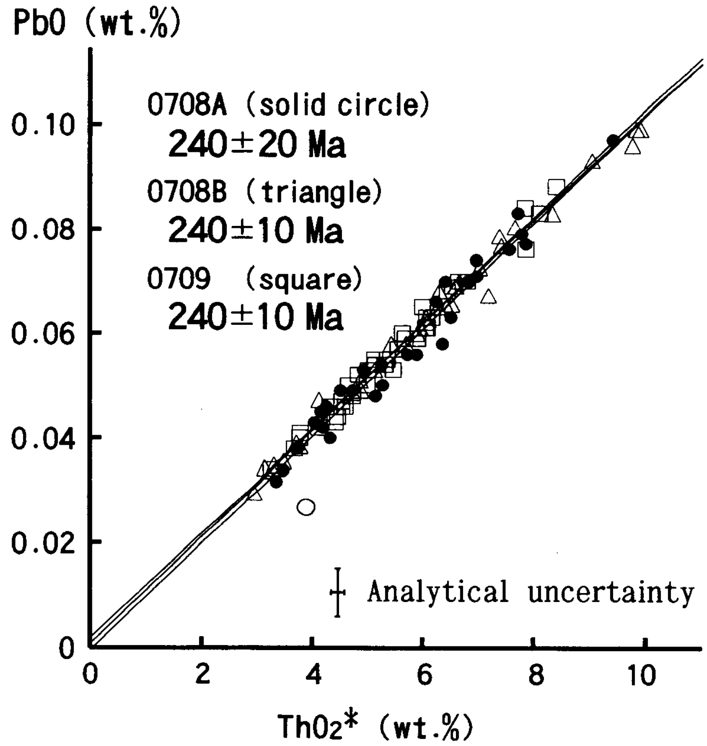

Fig. 4. Plots of PbO vs. ThO_2* for monazite grains from three adamellite samples (sample Nos. 0708A, 0708B and 0709) in the Hirasawa Mass. Open circle represents core of small grain M12 from sample 0708A. Error bars in the figure represent 2σ analytical uncertainty, and errors given to the age are of 2σ.

Zircon grains from sample 0708A contains ThO_2 and UO_2 up to 0.35% and 0.57%, respectively. The analytical data are given on the PbO-UO_2* diagram (Fig. 5). Data points (solid circle) for euhedral grains, except two (open circle) for the rim of grain Z10, are arrayed linearly in the diagram. The best-fitted isochron (MSWD=0.07) gives an age of 240±20 Ma with an intercept value of 0.0005±0.0008. The CHIME zircon age is identical within analytical error with CHIME monazite ages.

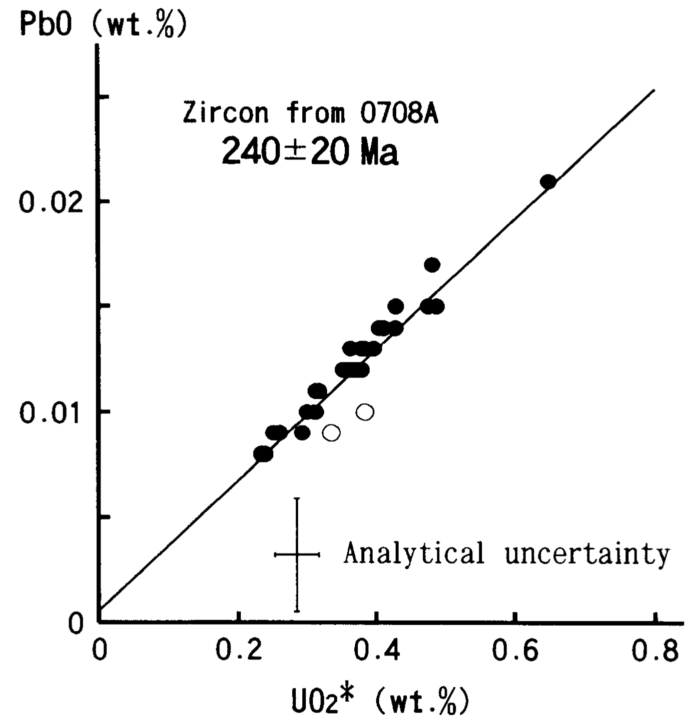

Fig. 5. Plots of PbO vs. UO_2* for zircon grains from adamellite sample 0708A in the Hirasawa Mass. Open circles represent rim of euhedral grain Z10. Explanation for errors is the same as for Fig. 4.

DISCUSSION

The CHIME monazite and zircon ages for the Hirasawa Mass coincide well with one another, concentrating at 240 Ma. This coincidence, together with the fact that some 240 Ma zircons show concentric growth zoning, strongly suggests that the CHIME ages represent the time of emplacement of the Hirasawa Mass. This clearly shows that the ca. 240 Ma Hirasawa Mass is not a pre-Silurian basement; nor is it correlative with the Carboniferous Hikami Granite that has a 351±12 Ma Rb-Sr whole-rock isochron age (Shibata, 1974) and 340–360 Ma CHIME ages (Suzuki and Adachi, 1991a; Suzuki et al., 1992). Our results are not coincident with the previous age assignment for these granitoid masses (e.g. Kitakami Paleozoic Research Group, 1982). Although late Permian to early Triassic plutonism has been inferred from K-Ar dating of granitoid clasts in the Usuginu Conglomerate (Shibata, 1973), no granitoid masses of this age have been identified in the South Kitakami terrane until our CHIME dating (Suzuki et al., 1992; Adachi et al., in press). Further CHIME geochronology on the leucocratic adamellite at Kusayami-zawa confirmed its emplacement in late Permian to early Triassic time. Analytical data of monazites from the adamellite (sample Nos. 1604 and 1605) are plotted on the PbO-ThO_2* diagram (Fig. 6). Eight data points (square) for single grain M01 from sample 1604 yield an isochron of 250±60 Ma (MSWD=0.13) with an intercept value of −0.0043±0.0158, and data points (solid circle) for sample 1605 yield an isochron of 250±10 Ma (MSWD=0.26) with an intercept value of −0.0015±0.0020.

Five data points (open circle) for grain M12 from sample 1605 lie below these isochrons and define a young isochron of 180 ± 50 Ma (MSWD=0.78) with an intercept value of 0.0069 ± 0.0234. The 180 Ma age is not uncommon for rims of monazite and zircon grains from other leucocratic adamellite at Kusayami-zawa (Suzuki et al., 1992). The late Permian to early Triassic plutonism and Jurassic thermal event must have occurred extensively in the South Kitakami terrane.

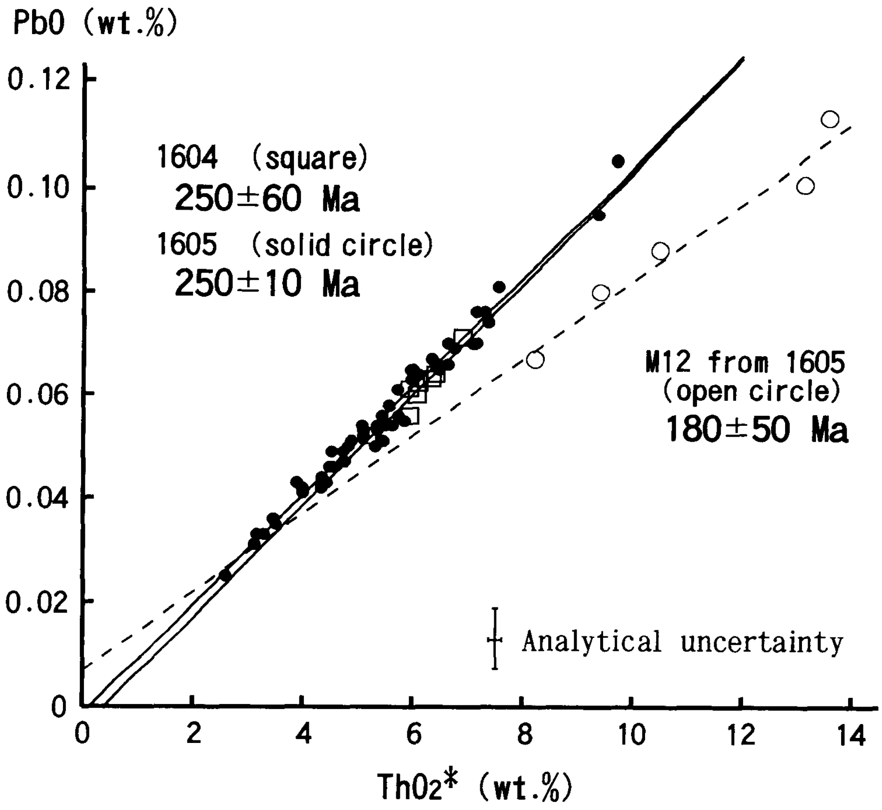

Fig. 6. Plots of PbO vs. ThO_2* for monazite from leucocratic adamellite (sample Nos. 1604 and 1605) collected at the mouth of the Kusayami-zawa. Analytical data are given in Appendix 2. Explanation for errors is the same as for Fig. 4.

Partial XRF analyses of samples 0708A and 0708B from Loc. 3 are shown in Table 1, together with the analytical data for the leucocratic adamellite at Kusayami-zawa and leucogranite from the Okuhinotsuchi Mass (Adachi et al., in press). Both the analytical results are nearly identical; samples 0708A and 0708B have 73.3 and 73.7% SiO_2, 1.50 and 1.49% CaO, K_2O/Na_2O ratios of 0.99 and 1.11, $CaO/(Na_2O+K_2O)$ ratios of 0.21 and 0.20, and molar $Al_2O_3/(CaO+Na_2O+K_2O)$ (A/CNK; hereafter) values of 1.12 and 1.06, respectively. Since magnetite and sphene are very rare or absent in the Hirasawa Mass, the rocks appear to bear many characteristics of the so-called ilmenite series (Ishihara, 1977) or S-type (White and Chappell, 1977) granite, although we prefer nongenetic term "peraluminous".

Table 1. Partial XRF analyses of adamellite samples from the Hirasawa Mass, together with chemical compositions of late Permian-early Triassic leucocratic adamellite at Kusayami-zawa and leucogranite of the Okuhinotsuchi Mass in the South Kitakami terrane (Adachi et al., in press).

	Hirasawa Mass		Kusayami-zawa			Okuhinotsuchi Mass					
	0708A	0708B	1603	1604	1605	1601A	1601B	1602A	1602B	0702	0703
SiO_2	73.3	73.7	74.8	75.5	75.2	77.2	78.4	73.8	79.7	76.7	76.5
TiO_2	0.22	0.22	0.25	0.24	0.25	0.06	0.04	0.17	0.10	0.05	0.07
Al_2O_3	13.8	13.7	13.1	13.0	12.9	12.3	11.7	13.6	10.7	12.3	12.8
FeO*	1.87	1.93	2.47	2.04	2.19	1.13	0.99	1.55	1.15	0.94	0.99
MnO	0.05	0.05	0.03	0.04	0.05	0.01	0.03	0.03	0.02	0.01	0.03
MgO	0.60	0.59	0.52	0.75	0.61	0.24	0.25	0.46	0.25	0.20	0.22
CaO	1.50	1.49	0.41	0.28	0.34	0.15	0.22	0.21	0.12	0.18	0.18
Na_2O	3.52	3.60	2.73	4.51	3.87	3.03	3.53	3.50	2.38	2.95	2.95
K_2O	3.49	4.00	4.04	2.31	3.18	4.79	3.48	5.22	4.78	4.77	5.11
P_2O_5	0.05	0.05	0.06	0.05	0.06	0.02	0.02	0.04	0.03	0.02	0.02
Total	98.40	99.33	98.41	98.72	98.65	98.93	98.65	98.58	99.23	98.12	98.87
A/CNK	1.12	1.06	1.36	1.25	1.24	1.18	1.17	1.15	1.15	1.20	1.19
K_2O/Na_2O	0.99	1.11	1.48	0.51	0.82	1.58	0.99	1.49	2.01	1.62	1.73
$CaO/(Na_2O+K_2O)$	0.21	0.20	0.06	0.04	0.05	0.02	0.03	0.02	0.02	0.02	0.02

FeO*: total Fe as FeO, A/CNK: molar $Al_2O_3/(CaO+Na_2O+K_2O)$ value.

Like the Hirasawa Mass, late Permian to early Triassic granitoids at Kusayami-zawa and from the Okuhinotsuchi Mass are also peraluminous; the A/CNK values are in the range between 1.24 and 1.36 for the leucocratic adamellite at Kusayami-zawa and in the range between 1.15 and 1.20 for the Okuhinotsuchi mass (Table 1). The similar A/CNK values for these late Permian-early Triassic granitoids imply their genetic relation. This inference is supported by a close similarity in zircon morphology (Fig. 7); most plots of length vs. elongation ratio for zircon grains from both the leucocratic adamellite at Kusayami-zawa and the leucogranite in the Okuhinotsuchi Mass fall within the data field for zircon grains from the adamellite in the Hirasawa Mass. However, differences in the ThO_2 content of monazite (Fig. 8) and the K_2O/Na_2O and $CaO/(Na_2O+K_2O)$ ratios suggest that they took independent paths of consolidation. Judging from the lower $CaO/(Na_2O+K_2O)$ ratios (0.02−0.03) and higher K_2O/Na_2O ratios (0.99−2.01, mostly larger than 1.5), the leucogranite of the Okuhinotsuchi Mass is regarded to be most differentiated among these granitoids. The leucogranite is also higher in SiO_2 (73.8−79.7%) and lower in TiO_2 (0.04−0.17%), FeO* (0.94−1.55%) and MgO (0.20−0.46%) than all other rocks. The leucocratic adamellite at Kusayami-zawa has lower $CaO/(Na_2O+K_2O)$ ratios (0.04−0.06), despite its high TiO_2 (0.24−0.25%), FeO* (2.08−2.47%) and MgO (0.52−0.75%) contents. It also shows exceptionally high A/CNK values (1.24−1.36) and variable K_2O/Na_2O ratios (0.51−1.48). Since silicate melt-silicate crystal equilibria generally constrain the A/CNK value to be 1.1−1.2 (Clarke et al., 1993), the leucocratic adamellite appears to be the products of hydrothermal alteration of a protolith which is more primitive than the adamellite in the Hirasawa Mass. The exceptionally high A/CNK values as well as the variable K_2O/Na_2O ratios are likely to have resulted from albitization and sericitization of plagioclase, observed under the microscope. The diversified chemical features among the Hirasawa Mass, the leucocratic adamellite at Kusayami-zawa and Okuhinotsuchi Mass can be interpreted in terms of some difference in their consolidation paths.

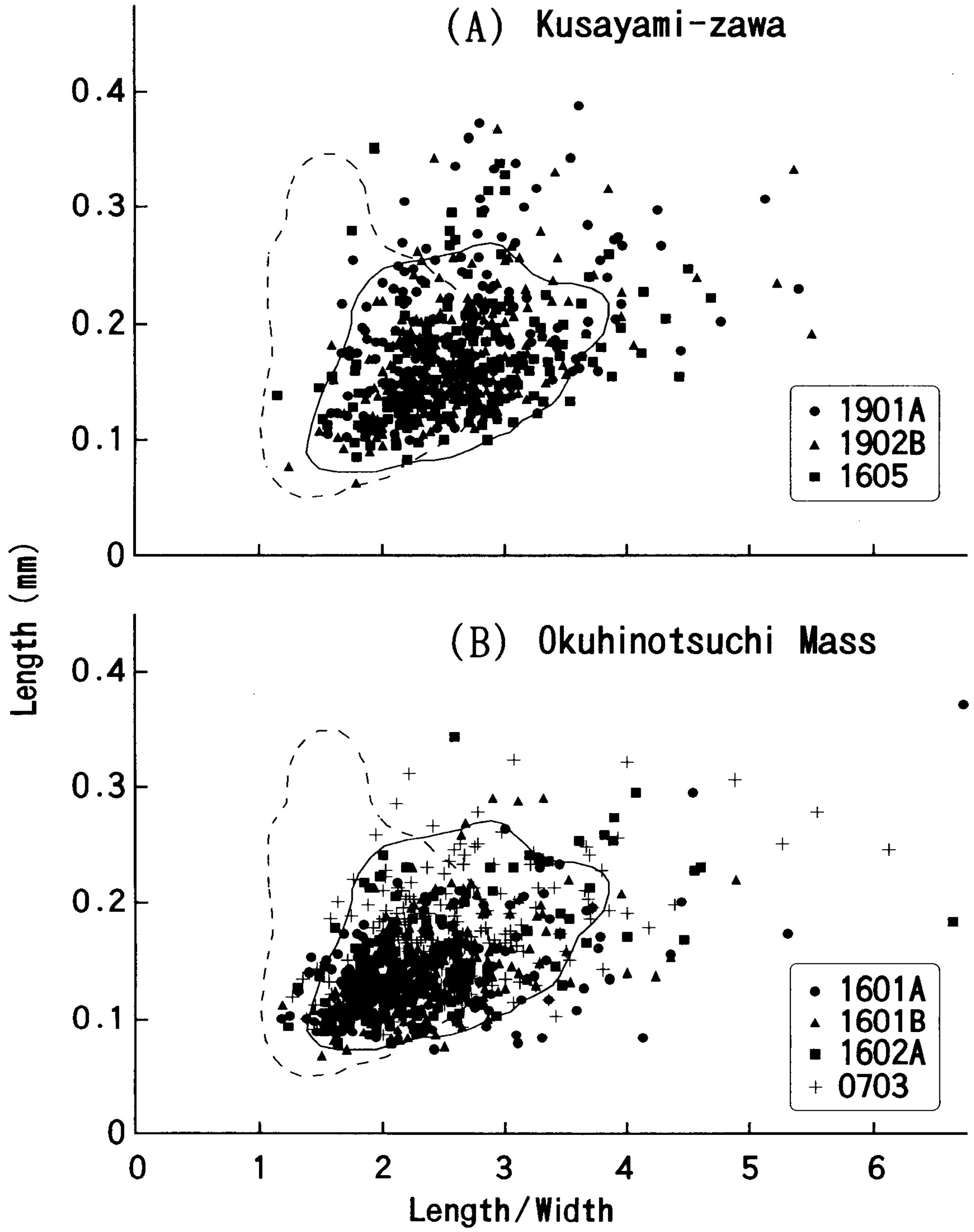

Fig. 7. Plots of length vs. elongation (length/width) for zircon grains from three samples (sample Nos. 1901A, 1902B and 1605) of leucocratic adamellite at Kusayami-zawa (A) and four leucogranite samples (sample Nos. 1601A, 1601B, 1602A and 0703) in the Okuhinotsuchi Mass (B). The solid and dashed lines define data fields for zircon grains from the Hirasawa Mass and the Cretaceous Kesengawa Granodiorite, respectively (see Fig. 3).

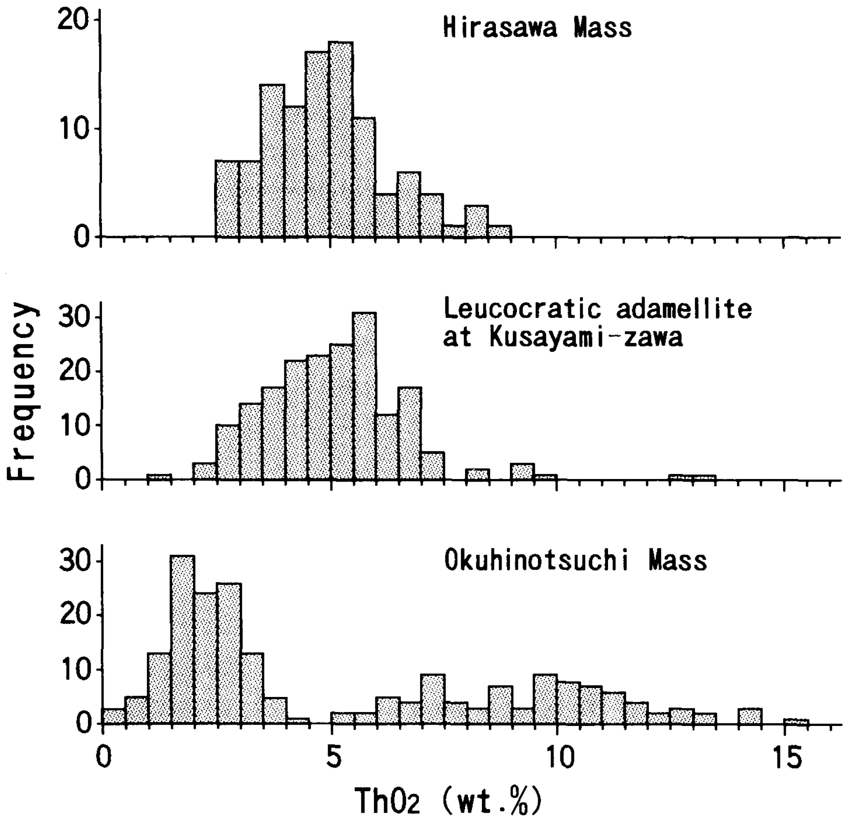

Fig. 8. Frequency distribution diagram of ThO_2 in monazite grains from adamellite in the Hirasawa Mass, leucocratic adamellite at Kusayami-zawa and leucogranite in the Okuhinotsuchi Mass. Th-rich monazite grains from leucogranite in the Okuhinotsuchi Mass, giving ca. 430 Ma CHIME age (Adachi et al., in press), are xenocrysts.

As demonstrated above, the late Permian to early Triassic plutonism in the South Kitakami terrane is not only extensive but also diversified. This plutonic activity may correspond to the major tectonic event related to the unconformity between the late Permian strata and the Triassic Inai Group of this terrane. The clastic sediments of the Inai Group and the overlying Jurassic Shizugawa Group contain a higher proportion of euhedral zircon grains as well as rock fragments of granitoids. The zircon grains, showing concentric growth zoning, high ThO_2 and UO_2 concentrations, and 240—280 Ma CHIME ages, suggest their derivation from the Hirasawa Mass, Okuhinotsuchi Mass, leucocratic adamellite at Kusayami-zawa or their correlatives.

Apart from the late Permian to early Triassic granitoids in the South Kitakami terrane, granitoids of similar age also occur sporadically in Southwest Japan: the Hida terrane (Suzuki and Adachi, 1991b), the Kanto mountains (Ono, 1983; Takagi et al., 1989; Hayama et al., 1990), the Todai Tectonic Zone (Shibata et al., 1993) and the Kurosegawa terrane (Shibata et al., 1979). Although most of these granitoids are diorite to granodiorite in composition and are characterized by low K_2O content, K_2O-rich ones with high SiO_2 contents occur as part of the "Gray Granite" in the Hida terrane. Our unpublished chemical data show that the Gray Granite ranges from 72.5 to 76.2% in the SiO_2 content, from 0.40 to 2.72 (largely over 1.6) in the K_2O/Na_2O ratio, from 0.98 to 1.07 in the A/CNK value and from 0.10 to 0.52 (largely below 0.15) in the $CaO/(Na_2O+K_2O)$ ratio. Furthermore, some varieties of the Gray Granite contain monazite and are free from sphene. These chemical and mineralogical features suggest that the monazite-bearing late Permian to early Triassic granitoids in the South Kitakami and Hida terranes appear to be cognate. This confirms our previous view that both the South Kitakami terrane in Northeast Japan and the Hida and circum-Hida terranes in Southwest Japan once shared a common geologic province (Adachi and Shibata, 1991; Suzuki and Adachi, 1991b; Adachi et al., in press).

CONCLUSIONS

The Hirasawa Mass previously regarded as a part of pre-Silurian basement in the South Kitakami terrane consists essentially of coarse-grained monazite-bearing adamellite that underwent, at least partly, contact metamorphism of the Cretaceous Kesengawa Granodiorite. The CHIME ages of magmatic monazite and zircon have revealed that the Mass was emplaced in late Permian to early Triassic time (240 ± 10 Ma). The granite, characterized by a higher K_2O/Na_2O ratio, is broadly similar to the late Permian to early Triassic leucogranite in the Okuhinotsuchi Mass and leucocratic adamellite at Kusayami-zawa, suggesting that the late Permian-early Triassic plutonism was much extensive. The late Permian to early Triassic CHIME ages require profound revisions in the regional tectonic framework and the Paleozoic-Mesozoic geologic evolution in the South Kitakami terrane.

ACKNOWLEDGEMENTS

We thank Professors S. Mizutani and K. Shibata of Nagoya University for their encouragement during the study. This work was supported in part by Grant-in-Aid for Fundamental Scientific Research (Nos. 03452068 and 04402016) from the Ministry of Education, Science and Culture, Japan.

REFERENCES

Adachi M. and Shibata K. (1991) A 254-Ma-old metagabbro intruding the Arakigawa Formation of the circum-Hida terrane, central Japan. *J. Earth Sci., Nagoya Univ.* **38**, 39–48.

Adachi M. and Suzuki K. (1992) A preliminary note on the age of detrital monazites and zircons from sandstones in the Upper Triassic Nabae Group, Maizuru terrane. *Mem. Geol. Soc. Japan* No. 38, 111–120 (in Japanese with English abstract).

Adachi M., Suzuki K., Yogo S., and Yoshida S. (in press) The Okuhinotsuchi granitic mass in the South Kitakami terrane: pre-Silurian basement or Permian intrusives. *J. Min. Pet. Econ. Geol.*

Clarke D.B., MacDonald M.A., Reynolds P.H., and Longstaffe F.J. (1993) Leucogranites from the eastern part of the South Mountain Batholith, Nova Scotia. *J. Petrology* **34**, 653-679.

Hayama Y., Shibata K., and Uchiumi S. (1990) K-Ar age of rocks from the northern margin of the Kanto Mountains. *J. Geol. Soc. Japan* **96**, 319–322 (in Japanese).

Ishihara S. (1977) The magnetite-series and ilmenite-series granitic rocks. *Mining Geol.* **27**, 293–305.

Kawamura M. (1983) The Silurian Okuhinotsuchi Formation and pre-Silurian granite mass in the southern Kitakami Mountains, Northeast Japan. *J. Geol. Soc. Japan* **89**, 99–116 (in Japanese with English abstract).

Kawano Y. and Ueda Y. (1964) K-A dating on the igneous rocks in Japan (II) – Granitic rocks in Kitakami massif –. *Sci. Rept. Tohoku Univ. Ser. III* **9**, 199–215.

Kitakami Paleozoic Research Group (1982) Pre-Silurian basement rocks of the South Kitakami belt. *Mem. Geol. Soc. Japan* No. 21, 261–281 (in Japanese with English abstract).

Metal Mining Agency of Japan (1971) Report on the regional survey, Tono district. Ministry Intern. Trade Industry, 35p (in Japanese).

Mori K., Okami K., and Ehiro M. (1992) Paleozoic and Mesozoic sequences in the Kitakami mountains. In *Paleozoic and Mesozoic terranes: basement of the Japanese island arcs* (ed. M. Adachi and K. Suzuki). 29th IGC field trip guide book, Vol. 1, 81–114.

Murata M., Kanisawa S., Ueda Y., and Takeda N. (1974) Base of the Silurian system and pre-Silurian granites in the Kitakami massif, Northeast Honshu, Japan. *J. Geol. Soc. Japan* **80**, 475–486.

Ono A. (1983) K-Ar age of the Kinshozan quartz diorite from the Kanto Mountains. *J. Japan. Assoc. Min. Pet. Econ. Geol.* **78**, 38–39 (in Japanese with English abstract).

Shibata K. (1973) K-Ar ages of the Hikami granite and the Usuginu granitic clasts. *J. Geol. Soc. Japan* **79**, 705–707 (in Japanese).

Shibata K. (1974) Rb-Sr geochronology of the Hikami granite, Kitakami mountains, Japan. *Geochem. J.* **8**, 193–207.

Shibata K., Takagi H., Inazaki T., and Uchiumi S. (1993) Granitic rocks and their radiometric ages from the Todai Tectonic Zone on the Aokuzure pass, Akaishi Range. *J. Geol. Soc. Japan* **99**, 135–144 (in Japanese with English abstract).

Shibata K., Uchiumi S., and Nakagawa T. (1979) K-Ar age results – 1. *Bull. Geol. Surv. Japan* **30**, 675–686 (in Japanese with English abstract).

Suzuki K. and Adachi M. (1991a) Precambrian provenance and Silurian metamorphism of the Tsubonosawa paragneiss in the South Kitakami terrane, Northeast Japan, revealed by the Th-U-total Pb chemical isochron ages of monazite, zircon and xenotime. *Geochem. J.* **25**, 357–376.

Suzuki K. and Adachi M. (1991b) The Th-U-total Pb chemical isochron ages of zircon and monazite from the Gray Granite of the Hida terrane, Japan. *J. Earth Sci., Nagoya Univ.* **38**, 11–38.

Suzuki K., Adachi M., Sango K., and Chiba H. (1992) Chemical Th-U-total Pb isochron ages of monazites and zircons from the Hikami Granite and "Siluro-Devonian" clastic rocks in the South Kitakami terrane. *J. Min. Pet. Econ. Geol.* **87**, 330–349 (in Japanese with English abstract).

Suzuki K., Adachi M., and Tanaka T. (1991) Middle Precambrian provenance of Jurassic sandstone in the Mino terrane, central Japan: evidence from an electron microprobe Th-U-total Pb monazite study. *Sediment. Geol.* **75**, 141–147.

Takagi H., Shibata K., Uchiumi S., and Fujimori H. (1989) K-Ar ages of granitic rocks in the northern marginal area of the Kanto Mountains. *J. Geol. Soc. Japan* **95**, 369–380 (in Japanese with English abstract).

White A.J.R. and Chappell B.W. (1977) Ultrametamorphism and granitoid genesis. *Tectonophysics* **43**, 7–22.

Appendix 1 Electron microprobe analyses of ThO_2, UO_2 and PbO of monazite and zircon from adamellite (sample Nos. 0708A, 0708B and 0709) of the Hirasawa Mass in the South Kitakami terrane. ThO_2*: sum of the measured ThO_2 and ThO_2 equivalent of the measured UO_2 for monazite, UO_2*: sum of the measured UO_2 and UO_2 equivalent of the measured ThO_2 for zircon.

Sample 0708-A (monazite)						Sample 0708-A (zircon)					
Grain No.	ThO2 (wt%)	UO2 (wt%)	PbO (wt%)	Age (Ma)	ThO2* (wt%)	Grain No.	ThO2 (wt%)	UO2 (wt%)	PbO (wt%)	Age (Ma)	UO2* (wt%)
M01-01	3.77	0.171	0.040	220	4.32	Z01-01	0.095	0.349	0.013	250	0.378
M01-02	3.79	0.143	0.046	260	4.25	Z01-02	0.041	0.305	0.011	260	0.318
M02-01	3.49	0.068	0.038	240	3.71	Z02	0.354	0.250	0.012	250	0.359
M02-02	4.67	0.079	0.053	250	4.93	Z03	0.051	0.297	0.011	260	0.313
M03-01	7.22	0.198	0.077	230	7.86	Z04-01	0.138	0.337	0.013	250	0.380
M03-02	4.00	0.157	0.049	260	4.51	Z04-02	0.076	0.210	0.008	250	0.233
M03-03	6.88	0.210	0.076	240	7.56	Z04-03	0.083	0.214	0.008	250	0.240
M04-01	4.27	0.145	0.049	250	4.74	Z04-03	0.075	0.270	0.009	230	0.293
M04-02	2.77	0.218	0.034	230	3.48	Z05-01	0.260	0.324	0.014	260	0.404
M05-01	3.81	0.108	0.045	260	4.16	Z05-02	0.102	0.456	0.015	230	0.488
M05-02	3.84	0.112	0.042	240	4.20	Z05-03	0.086	0.384	0.014	250	0.411
M05-03	5.01	0.605	0.074	250	6.97	Z05-04	0.033	0.369	0.012	230	0.379
M06-01	6.66	0.323	0.083	250	7.71	Z06-01	0.105	0.449	0.017	260	0.481
M06-02	6.27	0.165	0.070	240	6.80	Z06-02	0.134	0.434	0.015	230	0.475
M06-03	5.77	0.142	0.066	250	6.23	Z06-03	0.099	0.282	0.010	240	0.313
M06-04	4.71	0.134	0.048	220	5.14	Z07-01	0.056	0.243	0.009	250	0.260
M07-01	3.60	0.133	0.043	250	4.03	Z07-02	0.133	0.342	0.013	250	0.383
M07-02	2.93	0.131	0.032	230	3.35	Z07-03	0.098	0.340	0.012	240	0.370
M08-01	8.10	0.404	0.097	240	9.41	Z07-04	0.084	0.285	0.010	240	0.311
M08-02	4.70	0.170	0.054	240	5.25	Z08-01	0.106	0.364	0.013	240	0.397
M08-03	5.51	0.119	0.056	230	5.90	Z08-02	0.045	0.237	0.009	260	0.251
M09-01	4.80	0.480	0.058	220	6.35	Z09-01	0.249	0.572	0.021	240	0.649
M09-02	5.76	0.230	0.063	230	6.50	Z09-02	0.122	0.391	0.015	260	0.429
M10-01	4.38	1.05	0.079	240	7.78	Z09-03	0.109	0.394	0.014	240	0.428
M10-02	4.50	0.723	0.070	240	6.84	Z09-04	0.102	0.268	0.010	250	0.299
M10-03	4.54	0.751	0.071	240	6.97	Z10-01	0.134	0.321	0.013	260	0.362
M11-01	4.53	0.368	0.056	230	5.72	Z10-02	0.152	0.337	0.010	190	0.384
M11-02	4.95	0.448	0.070	260	6.40	Z10-03	0.129	0.312	0.012	250	0.352
M11-03	4.91	0.111	0.050	220	5.27	Z10-04	0.129	0.326	0.012	240	0.366
M12	3.55	0.105	0.027	160	3.89	Z10-05	0.066	0.315	0.009	200	0.335

Appendix 1 (continued)

Sample 0708-B (monazite)					
Grain No.	ThO2 (wt%)	UO2 (wt%)	PbO (wt%)	Age (Ma)	ThO2* (wt%)
M01-01	4.76	0.205	0.058	250	5.42
M01-02	5.49	0.319	0.065	240	6.52
M01-03	5.24	0.203	0.060	240	5.90
M02	3.02	0.088	0.035	250	3.31
M03-01	5.36	0.185	0.061	240	5.96
M03-02	5.16	0.344	0.065	250	6.27
M04-01	3.48	0.093	0.038	240	3.78
M04-02	6.57	0.140	0.073	240	7.02
M04-03	3.79	0.103	0.047	270	4.12
M04-04	3.37	0.107	0.039	250	3.72
M05-01	6.11	0.393	0.079	250	7.38
M05-02	7.05	0.396	0.083	240	8.33
M05-03	6.04	0.424	0.077	240	7.41
M05-04	5.95	0.383	0.067	220	7.19
M06-01	4.32	0.127	0.049	240	4.73
M06-02	5.89	0.169	0.065	240	6.44
M06-03	6.89	0.238	0.080	250	7.66
M07-01	2.70	0.078	0.030	240	2.95
M07-02	2.85	0.091	0.034	260	3.14
M07-03	2.97	0.162	0.036	240	3.49
M08-01	5.96	0.199	0.069	250	6.61
M08-02	5.88	0.130	0.068	260	6.30
M08-03	4.69	0.135	0.053	240	5.13
M09-01	5.42	0.198	0.063	250	6.06
M09-02	6.06	0.161	0.069	250	6.58
M09-03	5.13	0.175	0.058	240	5.70
M10-01	8.60	0.377	0.099	240	9.82
M10-02	7.95	0.560	0.096	230	9.76
M10-03	8.04	0.310	0.093	240	9.04
M10-04	8.27	0.506	0.099	240	9.91
M11-01	4.49	0.116	0.051	250	4.87
M11-02	5.50	0.180	0.062	240	6.08
M12-01	3.59	0.164	0.043	250	4.12
M12-02	4.63	0.079	0.049	240	4.89
M12-03	5.34	0.407	0.070	250	6.66

Sample 0709 (monazite)					
Grain No.	ThO2 (wt%)	UO2 (wt%)	PbO (wt%)	Age (Ma)	ThO2* (wt%)
M01-01	3.89	0.178	0.044	230	4.47
M01-02	4.81	0.170	0.055	240	5.36
M01-03	4.32	0.126	0.048	240	4.73
M02-01	3.91	0.157	0.046	250	4.42
M02-02	5.09	0.305	0.061	240	6.08
M02-03	5.04	0.293	0.065	260	5.99
M02-04	3.80	0.244	0.046	240	4.59
M02-05	4.23	0.237	0.050	240	5.00
M02-06	3.75	0.244	0.047	250	4.54
M02-07	3.34	0.239	0.042	240	4.11
M02-08	4.28	0.267	0.054	250	5.15
M03-01	7.31	0.337	0.088	250	8.40
M03-02	7.05	0.324	0.083	240	8.10
M03-03	5.49	0.355	0.070	250	6.64
M03-04	6.76	0.339	0.076	230	7.86
M04-01	3.26	0.159	0.040	250	3.78
M04-02	6.89	0.293	0.084	250	7.84
M04-03	2.82	0.133	0.034	250	3.25
M04-04	5.17	0.229	0.059	240	5.91
M05-01	4.41	0.283	0.054	240	5.33
M05-02	4.25	0.123	0.050	250	4.65
M05-03	4.56	0.140	0.053	250	5.01
M06-01	5.10	0.299	0.063	250	6.07
M06-02	3.75	0.245	0.046	240	4.54
M06-03	4.53	0.240	0.054	240	5.31
M07-01	5.01	0.192	0.060	250	5.63
M07-02	5.82	0.193	0.068	250	6.45
M07-03	5.12	0.132	0.057	240	5.55
M07-04	5.58	0.144	0.061	240	6.05
M08-01	4.67	0.143	0.055	250	5.13
M08-02	4.09	0.101	0.043	230	4.42
M08-03	3.97	0.106	0.046	250	4.31
M08-04	5.00	0.145	0.053	230	5.47
M08-05	4.46	0.114	0.052	250	4.83
M09-01	5.14	0.315	0.063	240	6.16
M09-02	4.91	0.239	0.059	250	5.68
M09-03	5.59	0.373	0.070	240	6.80
M09-04	3.06	0.192	0.038	240	3.68
M09-05	2.93	0.263	0.041	260	3.78
M09-06	5.40	0.350	0.069	250	6.53

Appendix 2 Electron microprobe analyses of ThO_2, UO_2 and PbO in monazites from leucocratic adamellite (Sample Nos. 1604 and 1605) at Kusayami-zawa in the South Kitakami terrane. ThO_2*: sum of the measured ThO_2 and ThO_2 equivalent of the measured UO_2.

Grain No.	ThO2 (wt%)	UO2 (wt%)	PbO (wt%)	Age (Ma)	ThO2* (wt%)
1604					
M01-01	5.69	0.113	0.060	230	6.06
M01-02	5.62	0.100	0.061	240	5.94
M01-03	6.00	0.106	0.063	240	6.34
M01-04	5.65	0.088	0.056	220	5.93
M01-05	6.60	0.090	0.071	240	6.89
M01-06	4.94	0.075	0.052	240	5.18
M01-07	6.19	0.066	0.064	240	6.40
M01-08	5.90	0.064	0.062	240	6.11
1605					
M01-01	5.99	0.109	0.067	250	6.34
M01-02	6.73	0.111	0.070	230	7.09
M01-03	6.31	0.100	0.066	240	6.63
M01-04	5.72	0.090	0.065	260	6.01
M02-01	4.57	0.097	0.051	250	4.88
M02-02	4.95	0.158	0.051	220	5.46
M03-01	3.83	0.158	0.042	230	4.34
M03-02	3.66	0.070	0.043	260	3.89
M03-03	5.21	0.093	0.054	230	5.51
M03-04	2.92	0.071	0.033	250	3.15
M04-01	4.19	0.075	0.043	230	4.43
M04-02	5.28	0.091	0.058	250	5.58
M04-03	4.11	0.074	0.044	240	4.35
M05-01	4.24	0.093	0.046	240	4.54
M05-02	3.05	0.072	0.033	240	3.28
M06-01	6.98	0.118	0.074	240	7.36
M06-02	6.42	0.103	0.069	240	6.75
M06-03	6.76	0.121	0.076	250	7.15
M06-04	5.68	0.088	0.065	260	5.97
M07	2.91	0.062	0.031	240	3.11
M08-01	5.07	0.076	0.050	220	5.32
M08-02	4.29	0.074	0.049	260	4.53
M09-01	6.97	0.102	0.076	250	7.30
M09-02	3.77	0.070	0.041	240	4.00
M10	5.55	0.091	0.055	220	5.84
M11-01	5.14	0.092	0.056	240	5.44
M11-02	3.32	0.055	0.035	240	3.50
M12-01	13.3	0.090	0.113	200	13.6
M12-02	8.05	0.052	0.067	190	8.22
M12-03	12.8	0.104	0.101	180	13.1
M12-04	9.18	0.072	0.080	200	9.41
M12-05	9.89	0.188	0.088	200	10.5
M13-01	3.70	0.087	0.042	250	3.98
M13-02	2.35	0.074	0.025	230	2.59
M14-01	3.15	0.098	0.036	250	3.47
M14-02	4.36	0.122	0.047	230	4.75
M14-03	5.33	0.124	0.061	250	5.73
M14-04	4.99	0.036	0.053	250	5.11
M14-05	4.08	0.121	0.046	240	4.47
M15-01	4.72	0.119	0.052	240	5.11
M15-02	5.39	0.106	0.056	230	5.73
M15-03	6.27	0.113	0.070	250	6.64
M15-04	6.77	0.118	0.070	230	7.15
M15-05	4.41	0.101	0.049	240	4.74
M16-01	5.66	0.140	0.064	250	6.11
M16-02	4.38	0.140	0.050	240	4.83
M17-01	7.24	0.096	0.081	250	7.55
M17-02	5.41	0.066	0.054	230	5.62
M17-03	6.22	0.078	0.065	240	6.47
M17-04	9.04	0.100	0.095	240	9.36
M17-05	9.40	0.098	0.105	260	9.72
M18-02	4.84	0.071	0.054	250	5.07
M18-02	3.30	0.049	0.036	250	3.46
M18-03	5.16	0.058	0.054	240	5.35
M18-04	4.57	0.077	0.050	250	4.82
M19-01	6.16	0.091	0.066	240	6.45
M19-02	5.68	0.089	0.063	250	5.97
M19-03	5.20	0.049	0.053	230	5.36